Incoherent Scatter Radar Simulator

John Swoboda

July 28, 2015

Chapter 1

Introduction

This report covers the physics, and signal processing used to create the incoherent scatter radar (ISR) simulator that is in the code base.

Chapter 2

ISR Spectrum

Overview

This is a description of the ISR spectrum process describes the mathematical basis for the software code base ISRSpectrum. It is based off of the development in [4] and [5] to form a spectrum.

Determining Spectra

The first step comes from [4] where a lumped circuit model is used to describe the spectrum. In it the independent thermal fluctuations of each species of ions and electrons are treated as current sources and the macroscopic conductances are treated as discrete components. The electric field E impinged from the radar acts as a voltage. This lumped circuit model, seen in Figure 2.1, is derived is taking the scalar component of Ampere's law in the direction of $\mathbf{k}$.

$$-j\mathbf{k}\times\mathbf{H}=\mathbf{J}+j\omega\epsilon_0\mathbf{E}, \tag{2.1}$$

which then yields,

$$0=(\sigma_i+\sigma_e)E+\frac{\omega}{k}e(n_{ti}-n_{te})+j\omega\epsilon_0 E. \tag{2.2}$$

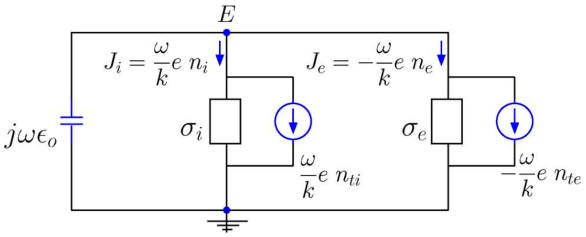

Figure 2.1: Lumped circuit model seen in [4].

Using the electron current expression, $-\omega k^{-1}en_e=E\sigma_e-\omega k^{-1}en_{te}$, these equations can be rearranged to solve for n_e,

$$n_e(\mathbf{k},\omega)=\frac{(j\omega\epsilon_0+\sigma_i)n_{te}(\mathbf{k},\omega)}{j\omega\epsilon_0+\sigma_e+\sigma_i}+\frac{\sigma_e n_{ti}(\mathbf{k},\omega)}{j\omega\epsilon_0+\sigma_e+\sigma_i}. \tag{2.3}$$

To determine the power spectrum we square and average Equation 2.3 taking into account that the terms n_{te} and n_{ti} are independent of one and other we result in the following

$$\langle|n_e(\mathbf{k},\omega)|^2\rangle=\frac{|j\omega\epsilon_0+\sigma_i|^2\langle|n_{te}(\mathbf{k},\omega)|^2\rangle}{|j\omega\epsilon_0+\sigma_e+\sigma_i|^2}+\frac{|\sigma_e|^2\langle|n_{ti}(\mathbf{k},\omega)|^2\rangle}{|j\omega\epsilon_0+\sigma_e+\sigma_i|^2}. \tag{2.4}$$

We can generalize them for multiple ion species by simply summing over the thermal fluctuations and conductances in Equation 2.2,

$$0 = \left(\sum_{k}^{K} \sigma_{ik} + \sigma_e\right) E + \frac{\omega}{k} e \left(\sum_{k}^{K} n_{tik} - n_{te}\right) + j\omega\epsilon_0 E. \tag{2.5}$$

This then augments the power spectrum in Equation 2.4 to the following

$$\langle |n_e(\mathbf{k},\omega)|^2 \rangle = \frac{\left|j\omega\epsilon_0 + \sum_k^K \sigma_{ik}\right|^2 \langle |n_{te}(\mathbf{k},\omega)|^2 \rangle}{\left|j\omega\epsilon_0 + \sigma_e + \sum_k^K \sigma_{ik}\right|^2} + \frac{|\sigma_e|^2 \left\langle \left|\sum_k^K n_{tik}(\mathbf{k},\omega)\right|^2 \right\rangle}{\left|j\omega\epsilon_0 + \sigma_e + \sum_k^K \sigma_{ik}\right|^2}. \tag{2.6}$$

Gordeyeve Integrals

The power spectrum of the thermal fluctuation for each species s can be determined by the following,

$$\frac{\langle |n_{ts}(\mathbf{k},\omega)|^2 \rangle}{N_0} = 2\mathrm{Re}\{J_s(\omega_s)\}, \tag{2.7}$$

where N_s is the average density for the species. Also the conductance for each species s can be determine from the following,

$$\frac{\sigma_s(\mathbf{k},\omega)}{j\omega\epsilon_0} = \frac{1 - j\omega_s J_s(\omega_s)}{k^2 \lambda_s} \tag{2.8}$$

where $\omega_s \equiv \omega - \mathbf{k}\cdot\mathbf{V}_s$ is the Doppler shifted frequency and $\lambda_s \equiv \sqrt{\frac{\epsilon_0 K T_s}{N_s q_s^2}}$ is the Debye length for each species.

The J_s terms can be represented as follows

$$J_s(\omega) \equiv \int_0^\infty \langle e^{j\mathbf{k}\cdot\Delta\mathbf{r}_s} \rangle e^{j\omega\tau} d\tau \tag{2.9}$$

These terms are known as Gordeyeve integrals, which are the one sided Fourier transforms of the characteristic functions of the particle displacements $\langle e^{j\mathbf{k}\cdot\Delta\mathbf{r}_s} \rangle$.

The particle displacement function can change depending on magnetic field and collisionality of the plasma. For the high latitude F-region in the ionosphere a case of general importance is one of a non-magnitized and collision less plasma, where $\Delta\mathbf{r} = \mathbf{v}\tau$ where τ is the time interval. Assuming a Maxwellian the PDF of one dimensional displacement is

$$f(\Delta r) = \frac{1}{\sqrt{2\pi\langle r^2 \rangle}} e^{\frac{-\Delta r^2}{2\langle r^2 \rangle}}. \tag{2.10}$$

The variance term $\langle r^2 \rangle$ can be represented as

$$\langle r^2 \rangle = \langle v^2 \rangle \tau^2 = \frac{K T_s}{m_s} \tau^2 \tag{2.11}$$

where T_s is the temperature of the species, K is Boltzmans constant and m_s is the mass of the species in kg. To simplify notation like in [4], we will refer to $\sqrt{K T_s / m_s}$ as C. Which yields the following single particle ACF,

$$\langle e^{j\mathbf{k}\cdot\Delta\mathbf{r}} \rangle = e^{-\frac{1}{2} k^2 C^2 \tau^2}. \tag{2.12}$$

To model collisions we use the term ν as the collision frequency for the species. If $\nu << kC$ then 2.12 can be used as the single particle ACF. If not the following must be used.

$$\langle e^{j\mathbf{k}\cdot\Delta\mathbf{r}} \rangle = e^{-\frac{k^2 C^2}{\nu^2}\left(\nu\tau - 1 + e^{-\nu\tau}\right)} \tag{2.13}$$

Lastly if one is to add a magnetic field to the equations the single particle ACFs must now take into a account the orientation of the magnetic field. The authors of [4] use the convention of breaking up the

Bragg vector $\mathbf{k}$ into two components, one parallel to the magnetic field, $k_\parallel$ and one perpendicular,$k_\perp$, as such, $\mathbf{k} = \hat{b}k_\parallel + \hat{p}k_\perp$. This yields the following formulation for the single particle ACF,

$$\langle e^{j\mathbf{k}\cdot\Delta\mathbf{r}} \rangle = e^{-\frac{1}{2}k_\parallel^2 C^2\tau^2} \times e^{-\frac{2k_\perp^2 C^2}{\Omega^2}\sin^2(\Omega\tau/2)}, \tag{2.14}$$

where the gyro frequency is $\Omega = qB/m$This formulation neglects the effects of collisions which if taken into account yields the following single particle ACF,

$$\langle e^{j\mathbf{k}\cdot\Delta\mathbf{r}} \rangle = e^{-\frac{k_\parallel^2 C^2}{\nu^2}\left(\nu\tau - 1 + e^{-\nu\tau}\right)} \times e^{-\frac{k_\perp^2 C^2}{\nu^2+\Omega^2}\left(\cos(2\gamma) + \nu\tau - e^{-\nu\tau}\cos(\Omega\tau - 2\gamma)\right)}, \tag{2.15}$$

where $\gamma = \tan^{-1}(\nu\Omega)$. The for the case with the magnetic field as one gets closer to being fulling perpendicular to $\mathbf{B}$ the single particle ACFs become much more narrow band, to the point of becoming delta functions in the frequency space. It is necessary to use other methods beyond numerical integration to determine the Gordeyeve Integrals. The authors of [9] get around this problem by making a PIC code to determine the particle statistics.

Computational Considerations

One of the main challenges to calculating the ISR spectrums is calculating the Gordeyeve integrals. The case with no collisions or magnetic fields can be done analytically using Dawsons integral. This can be done using the identity

$$jZ(\theta) = \int_0^\infty e^{-j\theta t} e^{-\frac{t^2}{4}} dt = \sqrt{\pi} e^{-\theta^2} - j2e^{-\theta^2} \int_0^\theta e^{t^2} dt. \tag{2.16}$$

Using the terms found in Equation 2.12, $\theta = \omega_s / \left(\sqrt{2}kC\right)$ and $t = \sqrt{2}kC\tau$.

For other cases where analytical calculation is not possible a numerical integration scheme from [13] is used. It is also possible to use a Chirp-z based algorithm that is shown in [7] from the experiences of the author the first technique converges faster. The technique used in [13] changes the variable of integration for integrals of the following form,

$$I = \int_a^b f(z) dz. \tag{2.17}$$

The technique changes the variable z in the following way,

$$z = \frac{1}{2}(a+b) + \frac{1}{2}(b-a)\mathrm{Erf}(g(t)), \tag{2.18}$$

where $g(t)$ is a function that is choosen so $g(t) \to \pm\infty$ as $t \to \pm\infty$ and $Erf(u)$ is

$$\mathrm{Erf}(u) = \frac{2}{\sqrt{\pi}} \int_0^u e^{-t^2} dt. \tag{2.19}$$

Discretizing and changing variables the integral in Equation 2.17 becomes the following sum

$$I = \sum_{n=-N}^{N} A_n f\left(\frac{1}{2}(a+b) + \frac{1}{2}(b-a)\mathrm{Erf}(g(nh))\right) \tag{2.20}$$

where,

$$A_n = g'(nh) e^{-g(nh)^2}. \tag{2.21}$$

Like in [13], $g(nh) = \sinh(nh)$ and the grid spacing h is the following,

$$h = \frac{1}{N} \ln(1.05\sqrt{2}N). \tag{2.22}$$

Lastly to avoid cases of divid by zero errors the main equations have to be rearrange slightly. First off because some ion species could have zero density Equation 2.8 uses the Debye length of the electron species,λ_e as follows

$$\frac{\sigma_s(\mathbf{k},\omega)}{j\omega\epsilon_0} = \frac{1 - j\omega_s J_s(\omega_s)}{k^2\lambda_e}\left(\frac{q_s T_e N_s}{q_e T_s N_e}\right). \tag{2.23}$$

Also, to avoid having to more calculations then necessary the $j\omega\epsilon_0$. terms of Equation 2.6 are moved around. Thus it becomes,

$$\langle |n_e(\mathbf{k},\omega)|^2 \rangle = \frac{\left|1 + \sum_k^K \frac{\sigma_{ik}}{j\omega\epsilon_0}\right|^2 \langle |n_{te}(\mathbf{k},\omega)|^2 \rangle}{\left|1 + \frac{\sigma_e + \sum_k^K \sigma_{ik}}{j\omega\epsilon_0}\right|^2} + \frac{\left|\frac{\sigma_e}{j\omega\epsilon_0}\right|^2 \left\langle \left|\sum_k^K n_{tik}(\mathbf{k},\omega)\right|^2 \right\rangle}{\left|1 + \frac{\sigma_e + \sum_k^K \sigma_{ik}}{j\omega\epsilon_0}\right|^2}. \tag{2.24}$$

2.1 Examples

We can see in Figure 2.2 examples of ISR spectrums from different ISR systems. The spectrums were generated using the the parameters values $N_e = 1e11$, $T_e = 3000^o$K and $T_i = 3000^o$K and the system parameter values seen in Table 2.1. The ion acoustic frequency f_{ia} for each system with the following plasma parameters its wavelength λ was calculated using the following formula,

$$f_{ia} = \frac{\lambda}{2}\sqrt{\frac{k_b T_e + k_b \gamma_i T_i}{M}}, \tag{2.25}$$

where M is the ion mass in kg, k_b is Botlzmann's constant and γ_i is the adiabatic index which is set to 3 in all cases.

Table 2.1: ISR System Parameters

System Name	f_0 in MHz	f_s in kHz	α in ^{o}
AMISR	449	50	70
Sondrestrom	1290	100	80
Haystack	440	50	65
Arecibo	430	50	45
Jicamarca	50	10	1

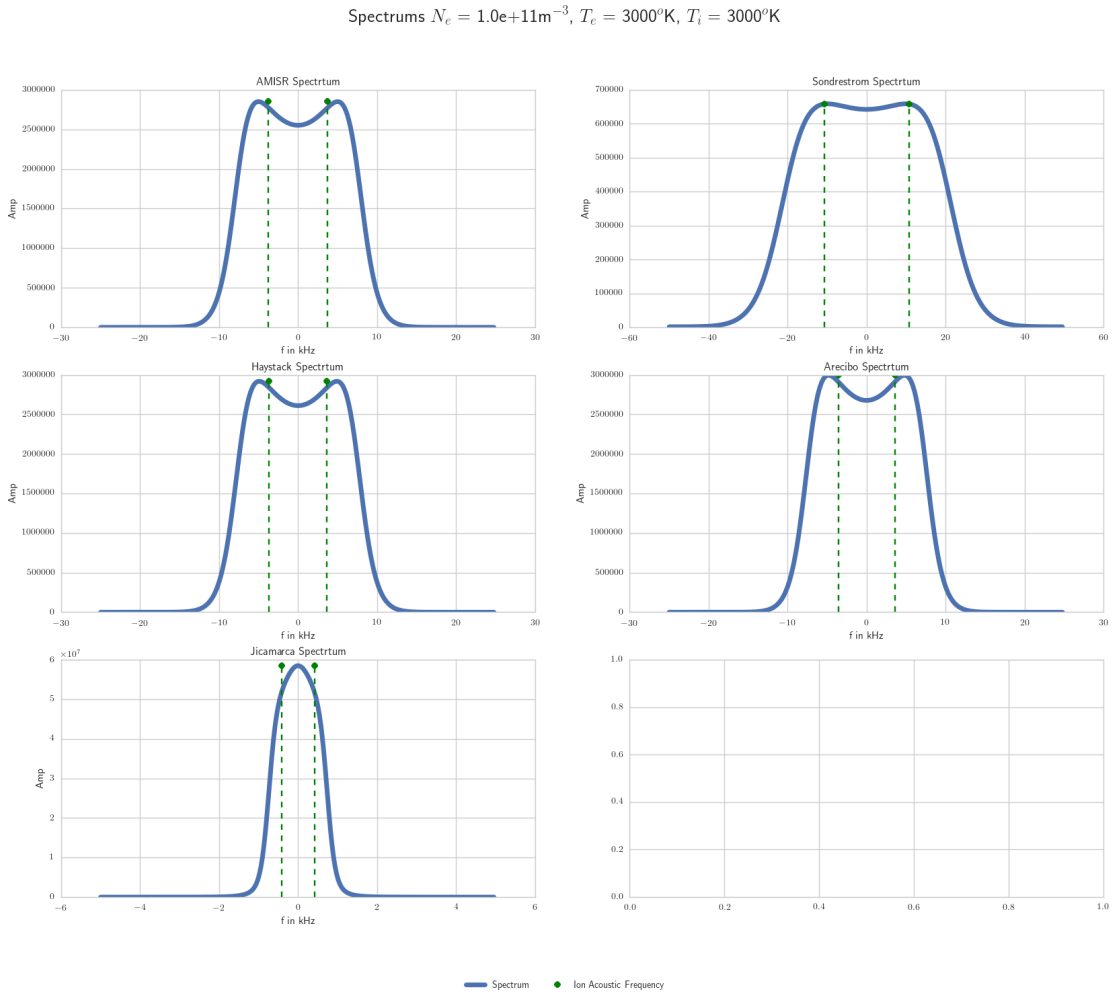

Figure 2.2: Spectrums From Different ISR Systems

Chapter 3

Data Formation

The 3-D ISR simulator creates data by deriving a time filter from the autocorrelation functions and applying them to complex white Gaussian noise generators. Stating this in another way, every point in time and space has a noise plant and filter structure as in Figure 3.1.

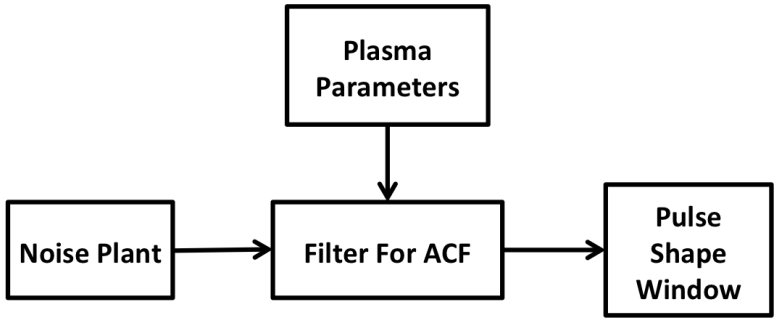

Figure 3.1: Diagram for I/Q simulator signal flow.

These filters are created using spatial averaging of an intrinsic ISR spectrum which come from the parameters at each point in space and space put into the simulator. The spatial averaging occurs by way of the antenna beam pattern, range gate size and pulse pattern. The beam pattern and range gate size act as an averaging across the range, azimuth and elevation dimensions of the intrinsic ISR spectrums. The pulse pattern acts as a windowing of the final samples of the data.

The simulator discretizes the ionosphere into a set of $m \in 0, 1, ...M-1$ range gates that have specific values of electron density (N_e), ion temperature (T_i), electron temperature(T_e), and masses of ion species (M_1 and (M_2)) that are present and their ratios (κ). The simulator creates a filter by taking the square root of the IS spectrum derived from a model,

$$H_m(\omega) = \sqrt{S_m(\omega |\, N_e, T_i, T_r, M_{i1}, M_{i2}, \kappa)}. \tag{3.1}$$

The filter can be created by taking the inverse Fourier transform of $H_m(\omega)$. Complex white Gaussian noise ($w(k) \sim CN(0,1)$) is then pushed though each of the filters and then windowed by the pulse creating the following:

$$y_m(k) = s(k)\left[h_m(k) * w(k)\right], \tag{3.2}$$

where $s(k)$ is the pulse shape. Currently in the the filtering is implemented by using the frequency response of the filter and multiplying by the complex noise and then inverse Fourier transforming it back. A diagram of a single noise plant can be seen in Figure 3.3

After the data for each range gate $y_m(k)$ is created the power of the return is calculated

$$P_r = \frac{cG\lambda^2}{2(4\pi)^2}\frac{P_t}{R^2}\frac{\sigma_e N_e}{(1+k^2\lambda_D^2),(1+k^2\lambda_D^2+T_r)} \tag{3.3}$$

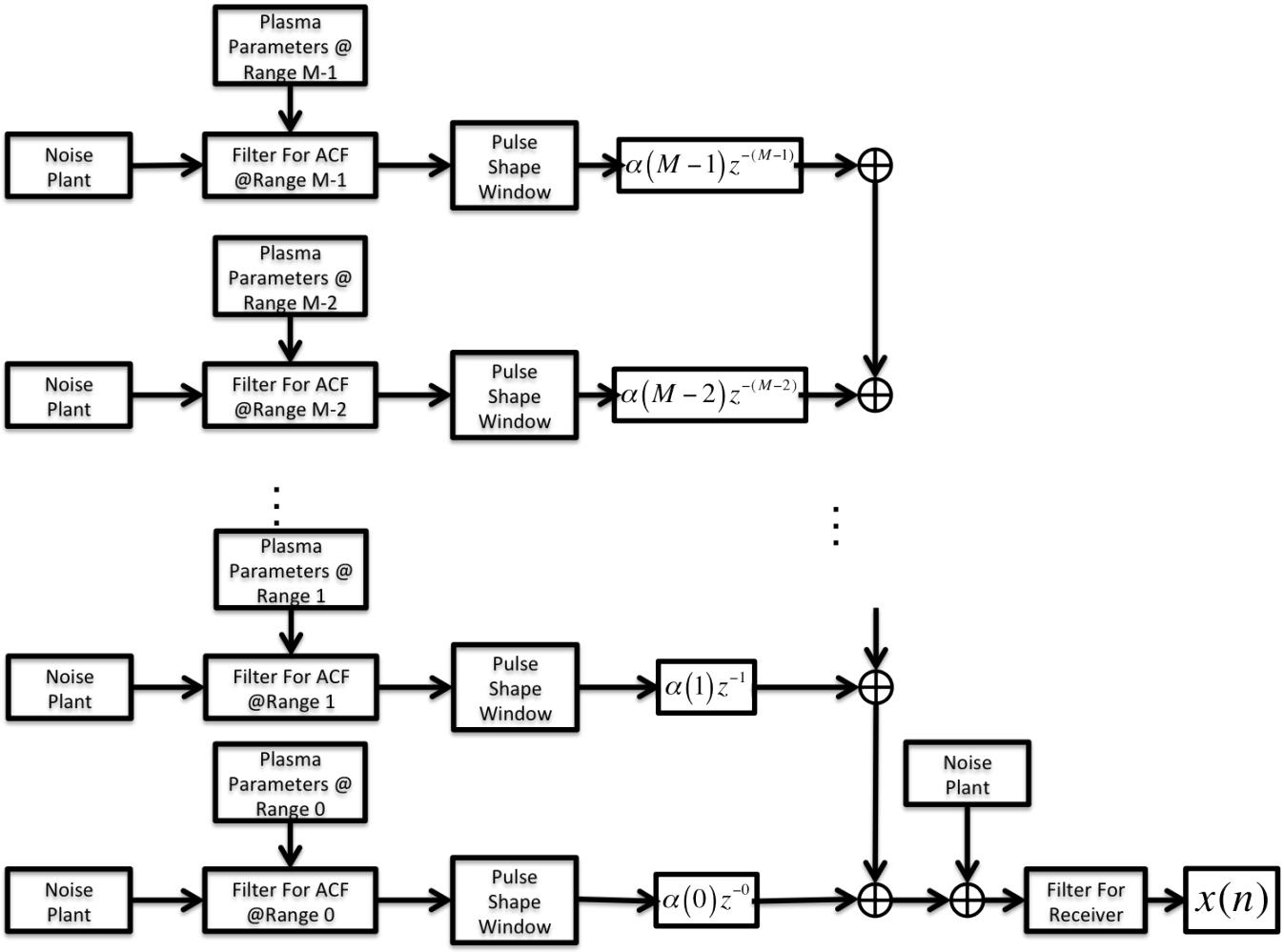

Figure 3.2: ISR Simulation Diagram

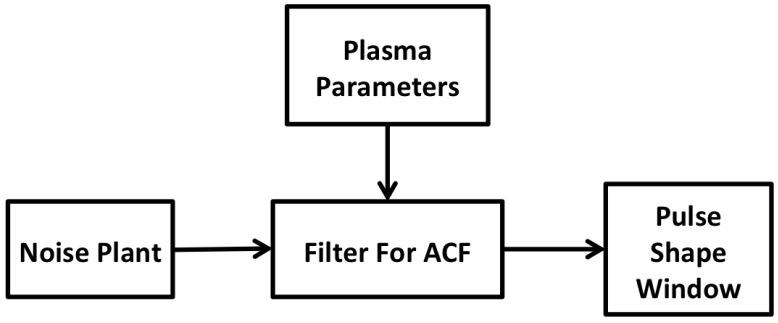

Figure 3.3: I/Q Simulator Diagram

where P_r is the power received, c is the speed of light, G is the gain of the antenna, P_t is the power of the transmitter, σ_e is the electron radar cross section, k is the wavenumber of the radar, λ_D is the Debye length and T_r is the temperature ratio.[1]

Once the power has been calculated for each range all of the data is delayed and summed together so as to model the arrival of the radar return at the receive:

[1]Currently all of the radar parameters used in the simulations are from the Poker Flat ISR system.

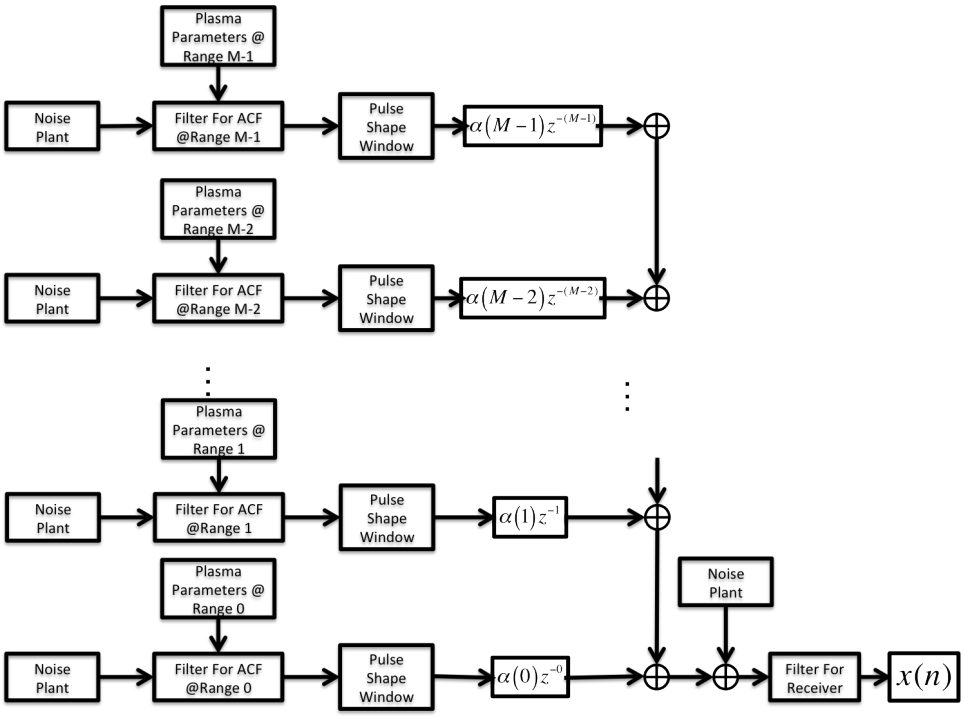

Figure 3.4: I/Q Simulator Diagram

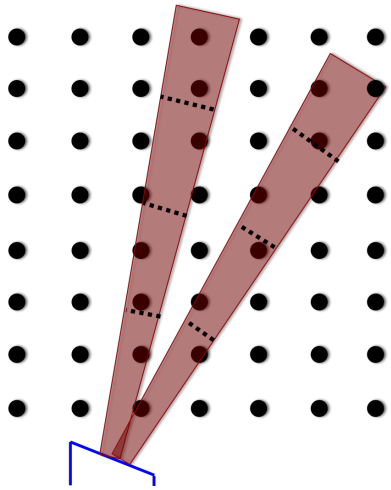

Figure 3.5: Beam Sampling Diagram

$$x(n) = \sum_{m=0}^{M-1} \alpha(m) y_m(n-m), \tag{3.4}$$

where $\alpha(m) = \sqrt{P_r(m)}$. A full diagram of the model can be seen in Figure 4.2.

The extension of this idea to three dimensional space takes the same concepts and repeats the process for multiple beams. The main differences is how the data is that the plasma parameters are first represented in Cartesian space. Each point will have a filter noise plant set up as seen in Figure 3.3. From there the data will be combined together with a weighting depending on the beam pattern. The data will then be delayed and weighted further depending on the range the point is located. A basic diagram can be seen in Figure 3.5.

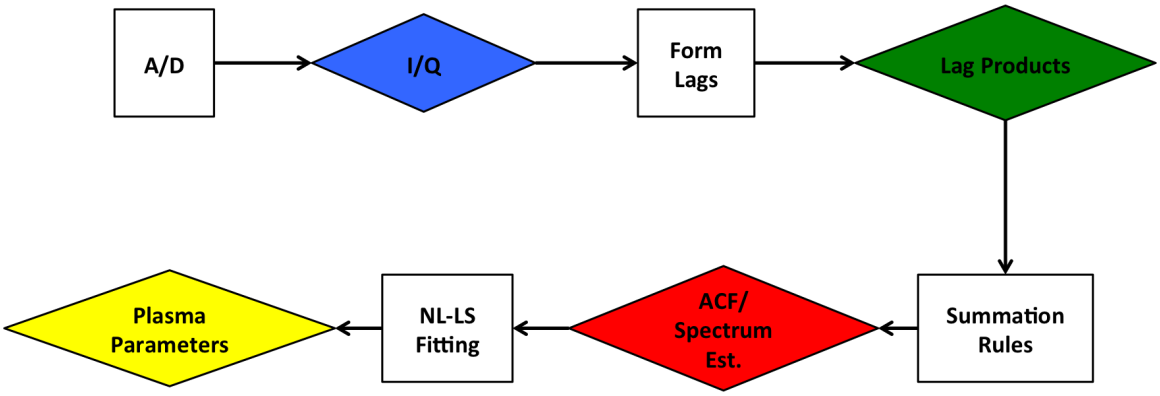

Figure 4.1: ISR signal processing chain, with signal processing operations as squares and data products as diamonds.

Chapter 4

ISR Processing

After the IQ data has been created it is processed to create estimates of the ACF at desired points of space. This processing follows a flow chart seen in Figure 4.1.

4.1 Lag Product Formation

The lag product formation is an initial estimate of the autocorrelation function. The sampled I/Q can be represented as $x(n) \in \mathbb{C}^N$ where N is the number of samples in an inter pulse period. At this point the first step in estimating the autocorrelation function is taken. For each range gate $m \in 0, 1, ...M-1$ an autocorrelation is estimated for each lag of $l \in 0, 1..., L-1$. To get better statistics this operation is performed for each pulse $j \in 0, 1, ...J-1$ and then summed over the J pulses. The entire operation to form the initial estimate of $\hat{R}(m, l)$ can be seen in Equation 4.2:

$$\hat{R}(m,l) = \sum_{j=0}^{J-1} x(m - \lfloor l/2 \rfloor, j) x^*(m + \lceil l/2 \rceil, j). \tag{4.1}$$

The case shown in Equation 4.2 is a centered lag product, other types of lag products calculations are available but generally a centered product is used. In the centered lag product case range gate index m and sample index n can be related by $m = n - \lfloor L/2 \rfloor$ and the maximum lag and sample relation is $M = N - \lceil L/2 \rceil$. This lag product formation is the first step in taking a discrete Wigner Distribution [1].

4.2 Summation Rules

Applying a summation rule is usually the next step in creating an estimate of the autocorrelation function. This is done to get a constant range ambiguity across all of the lags for long pulse experiment[12].

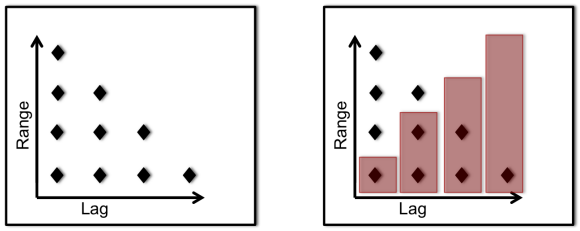

Figure 4.2: Summation Rule Diagram

The summation rule idea can be seen in Figure 4.2. In the figure the image on the left is a basic representation of an ambiguity function of a long pulse. Its mirrored on the right with red bars which would show the integration area under it so the ambiguity function will be of equal size in range.

In the processing this is basically a summing of lags from different ranges. The amount of summing is similar to what is shown in Figure 4.2. There are a number of different summing rule each with their own trade offs [12].

Lastly an estimate of the noise correlation is subtracted out of $\hat{R}(m,l)$, which is defined as $\hat{R}_w(m,l)$:

$$\hat{R}_w(m,l) = \sum_{j=0}^{J-1} w(m_w - \lfloor l/2 \rfloor, j) w^*(m_w + \lceil l/2 \rceil, j), \tag{4.2}$$

where $w(n_w)$ is the background noise process of the radar. Often the noise process is sampled during a calibration period for the radar when nothing is being emitted. The final estimate of the autocorrelation function after the noise subtraction and summation rule will be represented by $\hat{R}_f(m,l)$.

4.3 Nonlinear Least-Squares Fitting

After the final estimation of the spectrum is complete the nonlinear least squares fitting takes place to determine the parameters. The basic class of nonlinear least-squares problems as seen in [3], are shown in Equation 4.3,

$$\hat{\mathbf{p}} = \underset{\mathbf{p}}{\operatorname{argmin}} (\mathbf{y} - \boldsymbol{\theta}(\mathbf{p})) \boldsymbol{\Sigma} (\mathbf{y} - \boldsymbol{\theta}(\mathbf{p}))^*. \tag{4.3}$$

In Equation 4.3, the data represented as $\mathbf{y}$ would be the final estimate of the autocorrelation function $\hat{R}_f(m,l)$ at a specific range or its spectrum $\hat{S}_f(m,\omega)$. The parameter vector $\mathbf{P}$ would be the plasma parameters N_e, T_e, T_i and various other parameters including ion mass and ratios between different species. The fit function $\boldsymbol{\theta}$ is the IS spectrum calculated from models, such as once seen in [4], smeared by the ambiguity function. In the case of the long pulse the ambiguity can be simply applied by multiplying it with the autocorrelation function $R(l)$, if the summation rule is properly applied. Lastly the correlation matrix $\boldsymbol{\Sigma}$ if often realized as a diagonal matrix for many ISR systems. If it was not that would imply correlation with the measurement uncertainties between different lags or samples of the spectrum. The diagonal values usually used, noted as σ_i^2, usually the same unless there is a larger measurement error for one of the lags or spectrums. The following formula from [10] can be used:

$$\sigma_i = \frac{S}{\sqrt{J}} \left(1 + \frac{1}{SNR} \right). \tag{4.4}$$

where S is the signal power and SNR is the signal to noise ratio. These quantities can be estimated using the calibration period.

In the past ISR researchers have used the Levenberg-Marquart algorithm to fit data [11]. This specific iterative algorithm moves the parameter vector $\mathbf{p}$ by a perturbation $\mathbf{h}$ at each iteration[2]. Specifically Levenberg-Marquart was designed to be a sort of meld between two different methods Gradient Decent, and Gauss-Newton. The perturbation vector $\mathbf{h}_{lm}$ can be calculated using the following:

$$\left[\mathbf{J}^T \boldsymbol{\Sigma} \mathbf{J} \right] \mathbf{h}_{lm} = \mathbf{J}^T \boldsymbol{\Sigma} (\mathbf{y} - \boldsymbol{\theta}) \tag{4.5}$$

where $\mathbf{J}$ is the Jacobian matrix $\partial \boldsymbol{\theta} / \partial \mathbf{p}$ [6] [8]

Bibliography

[1] L. Cohen, *Time Frequency Analysis*. Prentice Hall, 1995.

[2] H. P. Gavin, "The levenberg-marquardt method for nonlinear least squares curve-fitting problems," 2013.

[3] S. Kay, *Fundamentals of Statistical Signal Processing, Vol. I - Estimation Theory*. Prentice Hall, 1993.

[4] E. Kudeki and M. Milla, "Incoherent scatter spectral theories: Part i: A general framework and results for small magnetic aspect angles," *IEEE Transactions on Geoscience and Remote Sensing*, vol. 49, no. 1, pp. 315–328, 2011.

[5] E. Kudeki and M. Milla, "Incoherent scatter spectrum theory for modes propagating perpendicular to the geomagnetic field," *Journal of Geophysical Research*, vol. 111, no. A6, p. A06306, 2006.

[6] K. Levenberg, "A method for the solution of certain non-linear problems in least squares," *Quarterly of Applied Mathematics*, vol. 2, pp. 164–168, 1944.

[7] Y. L. Li, C. H. Liu, and S. J. Franke, "Adaptive evaluation of the Sommerfeld-type integral using the chirp z-transform," *Antennas and Propagation, IEEE Transactions on*, vol. 39, no. 12, pp. 1788–1791, 1991.

[8] D. W. Marquardt, "An algorithm for least-squares estimation of nonlinear parmeters," *Journal of the Society for Industrial and Applied Mathematics*, vol. 11, pp. 431–441, Jun 1963.

[9] M. Milla and E. Kudeki, "Incoherent scatter spectral theories-part ii: Modeling the spectrum for modes propagating perpendicular to **b**," *IEEE Transactions on Geoscience and Remote Sensing*, vol. 49, no. 1, pp. 329–345, 2011.

[10] M. Nicolls, "Isr experiments data reduction and analysis." 2013.

[11] R. Nikoukar, F. Kamalabadi, E. Kudeki, and M. Sulzer, "An efficient near-optimal approach to incoherent scatter radar parameter estimation," *Radio Science*, vol. 43, no. 5, 2008.

[12] T. Nygren, *Introduction to Incoherent Scatter Measurements*. Invers OY, 1996.

[13] B. L. Ooi, "Useful integration quadrature for electromagnetics the Erf transform," *Microwave and Optical Technology Letters*, vol. 49, no. 4, pp. 789–791, 2007.